Graphite → diamond transition under high pressure: A kinetics approach

J. SUNG
China Grinding Wheel Corporation, Taipei, Taiwan; Taipei University of Technology, Taipei, Taiwan
E-mail: cgwrd@kinik.com

The graphite → diamond transition in the diamond stability field can be either direct or solvent-assisted. The direct transition may proceed by spreading a puckered basal plane of graphite in the direction perpendicular to it. The kinetics of such a transition may be approximated by the growth of a two-dimensional nucleus. The threshold temperature of the transition appears to depend on the degree of perfection of the original graphite. Hence, the more perfect the graphite is, the lower temperature it may transform into diamond. The solvent-assisted transition normally proceeds by rapid nucleation followed by growth of these nuclei. The kinetic model for continuous nucleation may be applied to the early stage of such transition. The activation energies for the transition can then be calculated. It is found that these activation energies seem to vary inversely with the solubility of carbon in these solvents at ambient pressure. Hence, the higher the amount of carbon a solvent dissolves at ambient pressure, the more effective it can be as a catalyst for the graphite → diamond transition under high pressure.

1. Introduction

1.1. Historical milestones of diamond synthesis

Until recent speculations of the author that carbon nitride (C_3N_4) and some other hypothetical structures may be harder than diamond [1], diamond has long been regarded as the hardest material.

As early as 1694 Florentine academicians already suspected that diamond was made of carbon when they found that the precious stone could be burned completely in air. This speculation was affirmed in 1772 by the French chemist Antoine Lavoisier. He discovered that the gas released from a burnt diamond was carbon dioxide. In 1797, Smithson Tennant proved beyond any doubt that diamond is made of carbon. He burnt a diamond in pure oxygen and measured the amount of carbon dioxide released. He found that the latter contained carbon that matched exactly the original weight of diamond [2]. As soon as the precious gem stone was known to be no more than ordinary carbon, the quest for synthesizing diamond began. But the success did not come until one and a half century latter.

The first artificial diamond was synthesized on February 15, 1953 by ASEA scientists of Sweden. The diamond was formed in a high pressure apparatus designed by Baltzar von Platen [3]. This apparatus was a complicated large cubic press that contained six anvils arranged in a shape of a split-sphere. The sample volume was over 4 cm^3, an enormous size at that time. The first diamond was produced from a mixture of iron carbide (Fe_3C) and graphite. The charge was compressed to a pressure of about 7.5 GPa and heated to a temperature of over 1500 °C for more than three minutes.

On December 16, 1954, Tracy Hall of General Electric Company in U.S.A. also synthesized diamond. He used a much simpler high pressure belt apparatus of his own design [4]. The sample volume had a meager size of less than 0.1 cm^3. It contained a mixture of troilte (FeS) and graphite. The sample was compressed to a pressure of about 7.0 GPa and heated to a temperature of about 1600 °C for two minutes. The diamond did not grow in the sample mixture as originally intended. Instead, it was embedded in the solid end cap made of tantalum. The end cap was used to lead the electric current to heat the sample.

The subsequent research of General Electric scientists led to the discovery that diamond could be formed at high pressure by the catalytic action of a molten metal. According to them, this metal must contain one or more elements selected from eight of Group VIIIa elements (Fe, Co, Ni, Ru, Th, Pd, Os, Ir, Pt) and three other transition metals (Mn, Cr, Ta) [5].

In 1961, diamond was converted directly from graphite without using a catalyst by du Pont's scientists [6]. The conversion was triggered by shock compression from an explosion that created momentarily (a few microseconds) a pressure of about 350 Kb and a temperature of about 770 °C. In 1963, the direct graphite → diamond conversion was also achieved by Francis Bundy of General Electric Company. This time the transition took place under a static pressure of about 12.0 GPa and a transient (a few milliseconds)

temperature of about 3000 °C. The temperature was raised by "flashing" the sample with a pulse of current suddenly released from a capacitor of high voltage [7].

In 1970, another milestone was reached when General Electric scientists announced the success in growing gem diamond [8]. The diamond was grown under precisely controlled pressure and temperature for extended periods of time. In order to avoid the pressure decay due to the volume reduction of the graphite → diamond transition, the carbon nutrient used was small diamond crystals themselves. These crystals were dissolved in a hot zone to provide carbon solutes that diffused to a cold region where they precipitated out onto a diamond seed.

In 1957, General Electric Company introduced the man-made diamond as superabrasives. Today, there are about 20 countries that are engaged in manufacturing diamond, of which China produced the most in quantity, but Ireland produced the most in quality due to the presence of both General Electric Company and De Beers Company. Each year over 300 tons of synthetic diamonds are produced under high pressure. These diamonds are indispensable for numerous industrial applications, such as drilling, sawing, grinding, lapping, and polishing of various materials (rocks, concretes, glass, ceramics, plastics, asphalts, non-ferrous metals . . . etc.).

There have been ample literature on diamond synthesis under high pressure. A comprehensive review on the high pressure technologies [9] for diamond synthesis and the mechanisms of diamond formation [10] are reported elsewhere. This mechanism may be contrasted by the formation of diamond metastably in liquid phase that was discovered in recent years [11]. Despite the extensive discussions of the graphite → diamond transition under high pressure, there have been very few papers [12, 13] that addressed the kinetics of this transition. In fact, there is no quantitative model that may describe the general behavior of the graphite → diamond transition. Moreover, there is not even a qualitative measure to account for various degrees of effectiveness of different catalysts. This paper is intended to fill up this gap by providing a systematic treatment of the kinetics of the graphite → diamond transition under high pressure. From this general treatment, the degrees of effectiveness of various catalysts may be quantitatively expressed and compared.

2. Kinetics of high pressure phase transitions

2.1. Kinetic models

For a phase transition without a compositional change, if the migration of atoms across the interface between the transforming phase and the transformed phase becomes rate limiting, nucleation and growth may soon approach a steady state, i.e., their rates are independent of time. In such a case, the kinetics of the phase transition may be described by the following listed equations [14].

When nuclei are formed freely, e.g., in a homogeneous medium, or in a heterogeneous medium when nucleation sites are not exhausted, the volume fraction of the transformed phase (F) is a function of nucleation rate (N), growth rate (G), and time (t) as follows:

$$F = 1 - \exp\left\{-\left(\frac{\pi}{3}\right)NG^3t^4\right\}. \tag{1}$$

When nucleation sites are exhausted, the transition will proceed mainly by the growth of existing nuclei. In such a case, F is no longer dependent on N, but on the concentration of existing nuclei. The latter may take a form of points (e.g., grain corners), lines (e.g., grain edges or dislocations), or surfaces (e.g., grain boundaries).

If there are C point nuclei per unit volume, then,

$$F = 1 - \exp\left\{-\left(\frac{4\pi}{3}\right)CG^3t^3\right\}. \tag{2}$$

If there are L length of line nuclei per unit volume, then,

$$F = 1 - \exp\{-\pi LG^2t^2\}. \tag{3}$$

If there are S area of surface nuclei per unit volume, then,

$$F = 1 - \exp\{-2SGt\}. \tag{4}$$

If existing nuclei are distributed uniformly with an average distance D between them, then C, L, and S my be estimated as:

$$C = \frac{12}{D^3}, \tag{5}$$

$$L = \frac{8.5}{D^2}, \tag{6}$$

and

$$S = 3.35/D. \tag{7}$$

The above equations are applicable for an interface-controlled diffusion. However, if the rate-limiting step of the transition is the diffusion of the atom in a matrix, then the kinetics may be expressed by a power law of time as:

$$F = Kt^a \tag{8}$$

Where K is proportional to the product of the diffusion coefficient of the atoms and the defect concentration of the transformed phase. The exponent a is determined by the mechanism of diffusion. The general pattern of F versus t for phase transitions of various modes as described above are compared in Fig. 1.

According to Sung [15], nucleation rate and growth rate under high pressure and temperature may be approximated by the following equations:

$$N = n\left(\frac{k}{h}\right)T\exp\left\{-\frac{(\Delta G^* + E_a)}{(kT)}\right\}, \tag{9}$$

and

$$G = \lambda\left(\frac{k}{h}\right)T\exp\left\{\frac{-E_a}{(kT)}\right\}\left\{1 - \exp\left[\frac{-\Delta G_a}{(kT)}\right]\right\}. \tag{10}$$

Where n is the number of nucleation sites per unit volume, k is Boltzmann's constant (8.62×10^{-5} eV/K), h is Planck's constant (4.14×10^{-15} eV-sec), T is temperature (K), ΔG^* is the activation energy of nucleation,

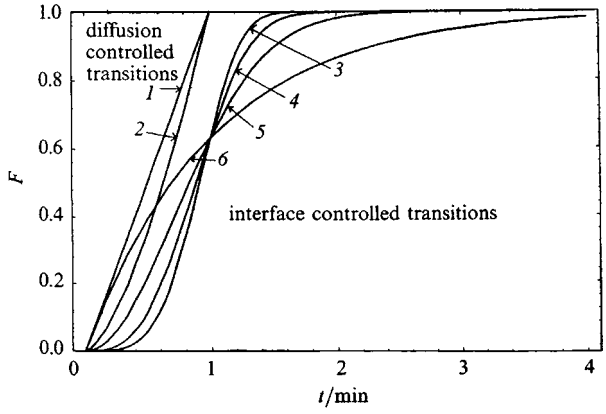

Figure 1 The dependence of the fraction (F) on time (t). Except for t, all variables in the equations are assumed to be unity so this diagram shows only the general shapes of the kinetic curves: *1*, $F = t$; *2*, $F = t^{3/2}$; *3*, $F = 1 - \exp(-t^4)$; *4*, $F = 1 - \exp(-t^3)$; *5*, $F = 1 - \exp(-t^2)$; *6*, $F = 1 - \exp(-t)$.

E_a is the activation energy of growth per atom, λ is the thickness of interface between the two phases, and ΔG_a is the driving force of the transition, i.e., the difference of free energy per atom between the transformed phase and the transforming phase.

$$\Delta G^* = \frac{(16\pi/3)\sigma^3}{(\Delta G + \xi)^2}, \tag{11}$$

$$\Delta G = \left(\frac{\Delta V}{V}\right)\Delta P,$$

and

$$E_a = E_0 + P\Delta V^*. \tag{12}$$

Where σ is the interface energy per unit area between the two phases, ξ is the strain energy per unit volume due to the structural mismatch between the two phases, ΔG is the driving force per unit volume, $\Delta V/V$ is the fractional volume change of the transition, E_0 is E_a at zero pressure, ΔV^* is the activation volume for growth, P is pressure, and ΔP is over-pressure, i.e., the excess pressure beyond the equilibrium boundary of the two phases for the transition.

The above described equations may be applied to the graphite → diamond transition. However, this transition may take many different routes, each with a unique set of energy barriers characteristic to a particular mechanism of transition. Moreover, these energy barriers are highly sensitive to catalysts chosen [10], hence, the applications of the above equations must be selective.

3. Mechanisms of direct graphite → diamond transition

3.1. Structural features of graphite and diamond

The four valence electrons in each carbon atom can form either $sp^2\pi$ bonds of graphite or sp^3 bonds of diamond. The former bonds are metal reinforced covalent bonds with a length of 1.45 Å. These bonds are stronger than pure covalent bonds of diamond that has a longer bond length (1,54 Å).

Each carbon atom in graphite can attach to three neighbors that lie on the same plane. Such a bonding structure allow atoms to form a network (0001) of carbon hexagons. Graphite contains layers of these networks that are loosely attached by weak van der Waals force with a separation distance of 3.35 Å at ambient pressure.

Each carbon atom in a graphite layer is surrounded by three neighbors. If every other carbon atom on a graphite layer is removed and the distance of the rest atoms are shortened, these remainder atoms will form a closest packed layer. In this case each atom will be surrounded by six neighbors instead of three. Such a layer is exactly the (111) plane of diamond.. In fact, diamond structure is made of such layers that form two interpenetrating closest packed lattices. Each lattice is located in the tetrahedral voids of the other lattice. This mixing lattice can be either hexagonal closest packed with AB... sequence of (0001) planes, or cubic closest packed with ABC... sequence of (111) planes. The former forms the structure of lonsdaleite (hexagonal diamond); and the latter cubic diamond. When graphite planes are collapsed to form diamond, the separation of closest packed planes is shortened from 3.35 Å of graphite to 2.06 Å of diamond.

When graphite transforms into diamond directly, each carbon atom with three neighbors must bridge across the matching atom in the adjacent layer to form a new bond. Such bonding can occur without breaking existing bonds with atoms of the same layer. However, in order to do so, each carbon atom must match the position with that of adjacent layers. The matching must be in such a way that every other atom on the same layer is aimed to one side of adjacent layer; and the rest atoms, the opposite side. During the transition, each of two halves of carbon atoms will form a closest packed lattice that resides in tetrahedral voids of the other.

Graphite layers can be stacked up in two different sequences: AB... (2H) or ABC... (3R). The former is known as hexagonal graphite; and the latter, rhombohedral graphite. The relative positions of carbon hexagons in these graphite is shown in Fig. 2. As seen from the figure, only half the amount of atoms in a layer of hexagonal graphite is matched with that in the adjacent layer. Thus, for 2H graphite to transform directly into diamond, it must first resequence to form 1H with A... or 3R with ABC... Such resequencing can take place martensitically by sliding specific layers in one bond length without long range diffusion. Such sliding is thermally activated, but it can be aided by applying shearing stress, or by contacting with a catalyst metal, such as Fe.

3.2. The puckering mechanism

Ordinary graphite contains a mixture of different layer sequences: about 85% in 2H and 15% in 3R. In order for 2H sequence to convert directly to diamond, it must first transform into either 1H or 3R. The direct conversion of the latter by puckering to corresponding structure of diamond is depicted in Fig. 3.

By analogy to carbon, direct phase transitions may also take place in boron nitride (1H), i.e., with CC

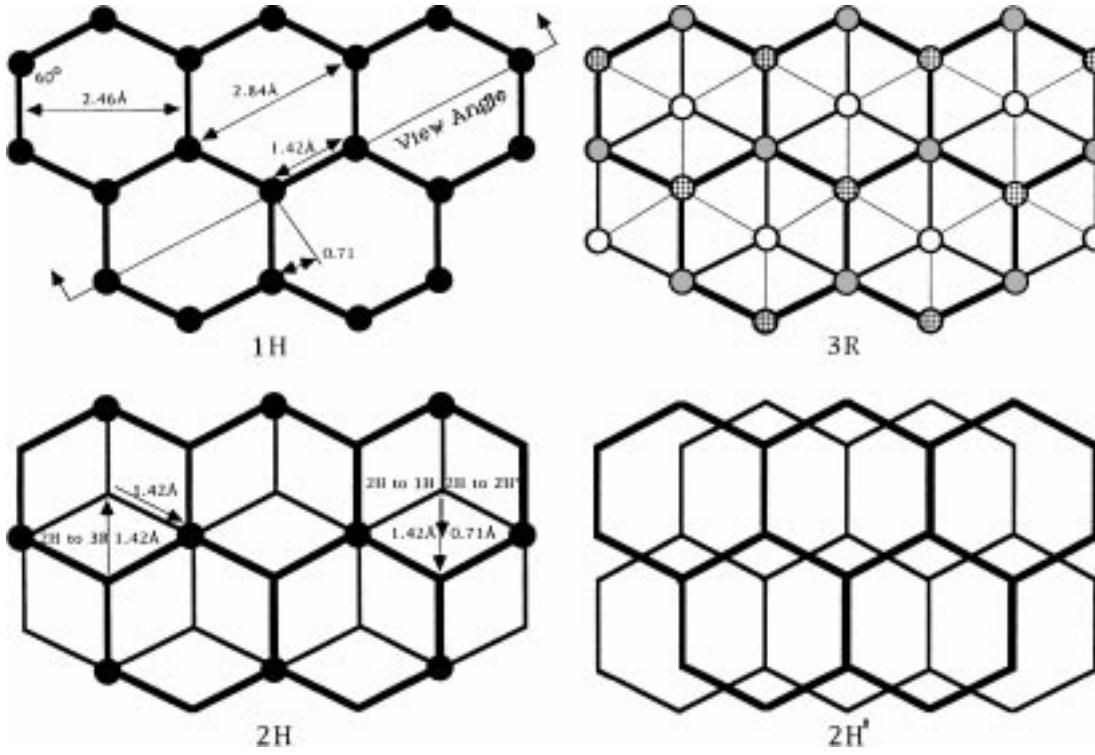

Figure 2 The Projection of Hexagonal Layers on the Basal Plane of Graphite. Each layer is denoted by different legend of line. 2H (hexagonal) graphite has a layer sequence of ABAB. 3R (rhombohedral graphite has a layer sequence of ABCABC. Note that in 2H graphite every other atom is matched with carbon atoms of adjacent layers, but the other half amount of atoms are not matched. However, all atoms in 3R graphite are matched with carbon atoms of adjacent layers (half with one side and other half with the other side). 2H and 3R sequences of graphite may transform into each other martensitically (without long range diffusion of carbon atoms) by sliding basal planes of one interatomic distance. 2H graphite may also convert to a metastable form of 1H graphite with AA... layer sequence. In this case, all atoms are matched with that of adjacent layers. The matching of carbon atoms with adjacent layers is a pre-requesite for the direct transition of graphite into diamond.

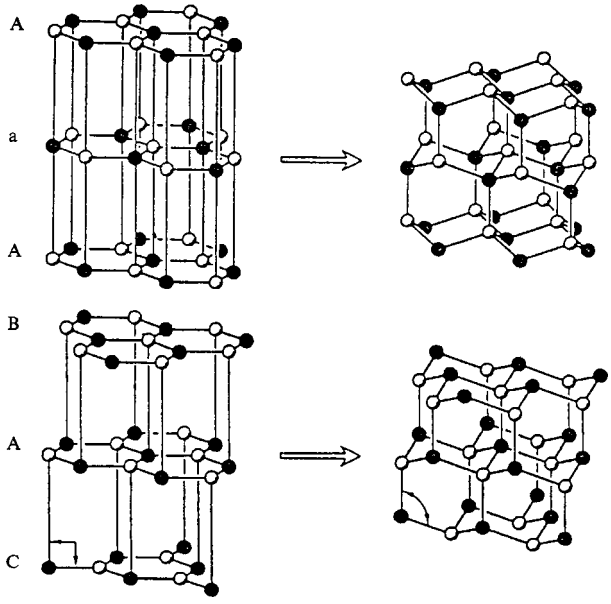

Figure 3 The Structural Changes of Graphite → Diamond Transition. The top diagram shows the direct transition of 1H metastable graphite (left) into 2H (hexagonal) diamond (lonsdaleite) (right). The bottom diagram shows the direction transition of 3R graphite (left) into 3C (cubic) diamond (right). Both transitions can take place by displasive movement of carbon atoms (puckering of graphite basal planes) without diffusion of carbon atoms. The majority graphite is 2H in sequence. It must first transform into 1H or 3H martensitically before converting to lonsdaleite (2H) or cubic diamond (3C), respectively. 2H diamond may also transform into 3C diamond martensitically. However, the activation energy is much higher as the separtion (2.06 Å at ambient pressure) between closest packed layers is much smaller than that (3.35 Å at ambient pressure) of basal planes in graphite.

replaced by BN [16]. The lattice parameters of corresponding phases between C and BN are within 2%. The mechanism of the direct hexagonal BN → cubic BN transition has been modeled by total energy calculations [17]. According to this model, as the matching atoms are approaching to each other under pressure from an initial distance of 3.34 Å, each basal layer of h-BN will remain flat until the distance is reduced to about 2.5 Å. At then, the basal layer will begin to pucker so the three $sp^2\pi$ bonds of each atom will gradually extend and bend away from the approaching atom. The puckering would incur an energy barrier that increases toward a maximum when the distance between the matching atoms is reduced to 2.2 Å. From then on, the angle between $sp^2\pi$ bonds would increase rapidly from an original 90 ° to approach 109.47 °, characteristic to sp^3 bonds. Total energy calculations predict that the activation energies (E_a) for such transition mechanisms at ambient pressure are 0.33 eV for C, i.e., graphite → diamond, and 0.19 for BN, i.e., h-BN → c-BN [18].

According to the above mechanism, the direct transition of either 1H → 2H, or 3R → 3C to diamond can be achieved by puckering of graphite bonds. When the puckering starts from a graphite separation of 3.35 Å at ambient pressure, the activation energy is at the maximum of about 0.33 eV. The activation energy for the graphite → diamond transition is proportional to the square of the separation between basal planes, hence, it will decrease with increasing pressure. For example, when the pressure is increased to 5, 10, 20, and 30 GPa;

the separation of basal planes will be reduced by 8.0%, 11.7%, 15.3%, and 17.1%; and the activation energy of puckering will be reduced to 0.28, 0.26, 0.24, 0.23 eV, respectively.

As the activation energy determines the threshold temperature of transition, therefore, the higher is the pressure, the lower temperature is required to trigger the transition. When the pressure is high enough to close the basal planes by about 1/3 (i.e., 2.20/3.35 or 34.3%) of their original separation, the activation energy for puckering graphite is reduced to zero. At such a pressure, the transition may become spontaneous.

3.3. Martensitic transitions in graphite

As discussed earlier, most graphite contains 2H sequence. It must first be transformed matensitically to either 1H or 3R sequence before it can be puckered into diamond structure. Such transitions do require short range displacement of carbon atoms by about one bond length (1.54 Å). Therefore, these transitions take time and they are thermally activated. Thus, the kinetics of the direct graphite → diamond transition may not be controlled by the athermal puckering process, but by the martensitic transition that takes place within graphite. This may be particularly true for the transition under very high pressure when the puckering becomes spontaneous.

If there is not enough time allowed for graphite to shuffle basal planes, such as that may occur during the shock synthesis of diamond by explosion, 2H graphite will remain unchanged. Only 3R graphite will form 3C diamond. In this case, the amount of diamond obtainable is dictated by the original proportion of 3R polytype. This explains why the conversion proportion of graphite during shock synthesis (e.g., produced by du Pont) is always low. Moreover, it was pointed out that if highly crystalline graphite was used as the source for shock synthesis, no diamond could be produced [6]. As highly crystalline graphite tends to be more in 2H sequence, such a structure is impossible to pucker into diamond structure without the intermediate form of 1H or 3R, the time is just too short for these transitional polytypes to form.

On the other hand, if the pressure can be sustained as in most cases of diamond synthesis, 2H graphite may slide into 3R graphite, and the latter converted readily into 3C diamond. This two-step process may explain why almost all diamonds formed by static compression are cubic forms. The only exception is the transition of large flakes of graphite. If these flakes are carefully oriented in perpendicular to the axis of compression so the shearing stress is minimized, 2H sequence may transform into 1H sequence upon heating. In this case, 2H diamond (lonsdaleite), instead of the normal cubic diamond, will be formed [19].

AB and ABC layers of graphite or diamond are identical in the first sphere of coordination; but they differ in the second. They can transform into each other by sliding every third layer along the same plane. Unlike reconstructive transitions that would require the breaking of all bonds, such martensitic transitions can proceed with the breaking of a smaller number (1/4 for graphite and 1/12 for diamond) of bonds.

The martensitic transition in graphite requires to break weak (0.075 eV at ambient conditions) van der Waal bonds, but it must overcome strong (3.69 eV at ambient conditions) covalent bonds of diamond. Hence, the martensitic transition in graphite from 2H → 3R occurs readily by shearing, e.g., by milling. However, the activation energy of this transition increases with pressure. Therefore, higher temperatures may be needed to aid the transition. Due to the much higher activation energy, the martensitic transition of 2H → 3C in diamond is extremely sluggish. It would require a much higher temperature to expedite such a transition.

3.4. The slope of phase boundaries

It may be possible to estimate the slope of the phase boundary for the AB → ABC transition of either graphite or diamond based on its possible changes of entropy and volume. The entropy change may be estimated from the configuration of atoms in a crystal structure [20]. According to the statistical thermodynamics, the entropy S is proportional to the number (W) of ways for arranging atoms in the crystal structures as follows:

$$S = S_0 + k \ln W \tag{13}$$

As the number of atoms required to specify AB sequence is only 2/3 of that for ABC sequence, hence the former is more ordered and with a lower entropy relative to the latter. Consider the entropy for arranging one gram of carbon atoms ($g = A/12$, where A is Avogadro' number) in AB sequence, $S = S_0 + k \ln 2^g$, whereas, it is $S = S_0 + k \ln 3^g$ for ABC sequence. Hence, the entropy change for the AB → ABC transition is approximately: $\Delta S = gk \ln 3/2$ or about 0.69 J/(gK) or 8.6×10^{-5} eV/K.

The distance of identical layers in AB sequence is also 2/3 of that for ABC sequence. As a result, the electrostatic repulsion force between every other layer in the former structure is likely higher than that in the latter (0.49% larger based on ab initio psdudopotential of local orbital method, [21]). Consequently, the structure of AB sequence may have a slightly larger volume than that of ABC sequence. Due to the shielding effect of electrostatic force, this volume difference is very minimal, in the order of 0.1%. Thus, $\Delta V = -4.4 \times 10^{-4}$ cm^3/g for graphite with a density of 2.26 g/cm^3, and $\Delta V = -2.8 \times 10^{-4}$ cm^3/g for diamond with a density of 3.52 g/cm^3.

The density of high temperature phase α-SiC (4H) is 3.208 g/c.c.; and low temperature phase β-SiC (3C), 3.210 g/c.c. Hence, for SiC, $\Delta V = -0.000623$ (0.06%) for AB → ABC transition.

For cubic diamond, (111) layers (002) are separated by 2.06 Å. But for lonsdaleite, it is 2.08 Å, about 1.1% larger. However, the perpendicular direction (i.e., a axis) is reduced by 0.36%, so the volume is about 0.40% larger [22].

d (002) is 1.2% longer, but a axis is –0.28% shorter, so the volume is 0.68% larger [23].

According to the above analysis, the AB → ABC transition of either graphite or diamond would have opposite signs in changes of entropy (ΔS) and volume (ΔV). If both sequences are stable, the slope of their phase boundary, i.e., $dP/dT = \Delta S/\Delta V$, would be negative, being approximately −16 Kb/°C for graphite and −25 Kb/°C for diamond. Due to the relative large entropy change and relative small volume changes, these phase boundaries are running about perpendicular to that of the graphite → diamond equilibrium line.

It has been reported that at ambient temperature, graphite will transform into a hexagonal phase above a pressure of 14–22 GPa [23]. However, unlike lonsdaleite (hexagonal diamond), this hexagonal phase is non-quenchable, so it will revert back to graphite upon decompression.

It is proposed that this mysterious hexagonal phase has an intermediate structure between graphite and lonsdaleite [24]. As discussed before, most graphite has a basal plane sequence of 2H. Therefore, only half of C atoms have matching counterparts from the adjacent layer. Unless the sequence of 2H is shuffled to either 1H or 3R that allow all atoms to match with adjacent layers (Fig. 3), diamond cannot be formed.

When pressure is high enough, C atoms with matching counterparts would form diamond bonds (sp^3). At ambient temperature, there is not enough thermal energy to shuffle 2H sequence. As a result, only half of C atoms can bridge across basal planes to form diamond bonds. The other half C atoms have no matching counterparts from adjacent layers, so they would retain graphite bonds ($sp^2\pi$). Such an intermediate structure between 2H graphite and 2H diamond is intrinsically unstable. Hence, it would revert readily back to 2H graphite upon decompression.

According to the above model, if the intermediate phase is heated under pressure, the unmatched C atoms could move to 1H locations where they can find matching atoms across basal planes to form diamond bonds (top diagram of Fig. 3). Such a structure is essentially lonsdaleite that is quenchable. Indeed, it was found that when the unquenchable phase was heated under pressure to a temperature exceeding about 800 °C, lonsdaleite could be preserved indefinitely upon decompression [19, 23].

The above model is consistent with the seemingly contradictory observations that the non-quenchable phase possess an X-ray diffraction pattern similar to lonsdaleite [23] yet its Raman spectra carry unmistakable signature of graphite ($sp^2\pi$) bonds [25]. The lonsdaleite structure is based on half bonded 2H sequence, and the graphite bonds comes from unmatched C atoms.

4. Kinetics of direct graphite → diamond transition

4.1. Parameters for the calculation

For a direct graphite → diamond transition, the interface thickness (λ) is about 2.4 Å, or about the average distance between the transformed diamond (1.54 Å) and transforming graphite (3.35 Å). This is also the distance when the energy is the highest between the two phases. At high pressure, the interface thickness is reduced, in the following calculations of the kinetics of graphite → diamond transition, we have assumed that this thickness is 2 Å.

The equation of graphite → diamond phase boundary is determined based on data summarized by Berman [26]. The data are taken from a temperature range most applicable for diamond synthesis (600 °C to 1700 °C). The equation has the following form:

$$P(\text{kb}) = 12.0 + 0.0301T(^\circ\text{C}) \qquad (14)$$

This equation is different from a more general phase boundary proposed by Kennedy and Kennedy [27] with the form:

$$P(\text{kb}) = 19.4 + 0.0250T(^\circ\text{C}) \qquad (15)$$

It should be noted that Equation 15 under-estimates the transition pressures (e.g., 13 Kb instead of 20 Kb at room temperature) relative to Equation 16 at lower temperatures as the slope (dP/dT) of the phase boundary tends to decrease with decreasing temperature.

The atomic volume of diamond at ambient conditions is 5.68 $Å^3$ (density 3.515 g/cm^3); and graphite, 8.78 $Å^3$ (density 2.265 g/cm^3). The fractional volume change for the transition at ambient conditions is −0.353 (the reverse transition is 1.546). The volume change, $\Delta V = V_{\text{diamond}} - V_{\text{graphite}}$, at the transition pressure and temperature can be calculated based on known effects of pressure and temperature on volume.

The volumes of diamond and graphite at a given pressure is estimated by the following simplified Birch-Murnaghan equation of state [28–30]:

$$P = 3B_0\left(\frac{V_0}{V}\right)^{5/3}\zeta(1 + a\zeta)$$

$$\zeta = (1/2)\left(\frac{V_0}{V}\right)^{2/3} - 1).$$

$$a = (3/2)(B_0' - 4)$$

Where V_0 and B_0 are volume and bulk modulus at zero (ambient) pressure; and B_0', the pressure derivative of the bulk modulus. For diamond, $B_0 = 4430$ Kb, $B_0' = 4$; and for graphite, $B_0 = 511$ Kb, $B_0' = 8.9$.

The temperature effect of volume can be estimated from:

$$V = V_0 + \int \alpha_T \, dT$$

Where V_0 is room temperature volume; and α_T, thermal expansion coefficient. For temperatures up to 2000 °C, the volume of diamond as a function of temperature is approximated by:

$$V_T(\text{cm}^3/\text{mole}) = 3.41 - 6.21 \times 10^{-6}T(^\circ\text{C}) + 2.33 \times 10^{-8}T(^\circ\text{C})^2,$$

and the volume of graphite as a function of temperature is approximated by:

$$V_T(\text{cm}^3/\text{mole}) = 5.30 - 3.15 \times 10^{-5}T(^\circ\text{C}) + 2.00 \times 10^{-8}T(^\circ\text{C})^2.$$

Based on the above parameters of bulk moduli and thermal expansion coefficients, the volume change of graphite → diamond transition may be expressed by:

$$\Delta V(\mathrm{cm}^3/\mathrm{mole}) = -1.89 - 3.77 \times 10^{-5} T(^\circ\mathrm{C}) + 3.23 \times 10^{-9} T(^\circ\mathrm{C})^2 + 5.60 \times 10^{-3} P(\mathrm{Kb})$$

4.2. Results of the calculation

The literature data on the kinetics of the direct graphite → diamond, transition under static compression are summarized in Table I. Most data indicate that the transition took place at a considerable (>3 GPa) over-pressure. As the result of such a high degree of metastability, the nucleation often proceeded almost instantaneously throughout the entire sample. Moreover, as suggested by Fig. 3, the nuclei could take the form of a puckered surface. As a result, the transition may be approximated by the simultaneous growth of saturated nuclei of two-dimensional surface. Hence, Equations 4 and 7 may be applicable.

Due to the explosive nature of the direct transition, the diamond crystals formed were typically microscopic crystallites. In the following calculation, it is assumed that the diameter of the puckered nuclei is about the size of these crystallites as listed in Table I. Based on such an assumption, the activation energies for the direct graphite → diamond transition are estimated and listed in Table I. It should be noted that these activation energies are for the slower processes of martensitic shuffling of graphite layers and the puckering motions of corrugated surfaces.

TABLE I Kinetic data of the direct graphite to diamond transition under static compression. Notes: the numbers in brackets are estimated; *f* is flush heating; *c* is current heating; *r* is room temperature without heating; type C is cubic diamond; type H is hexagonal diamond (lonsdaleite); *F* is the degree of transition (volume fraction of the transformed phase); *E* is the activation energy of growth for the transport of atoms across the interface

C source	Reference	Heating (*f*, *c* or *r*)	*p*/kbar	Overpressure/kbar	*T*/°C
SP-1 graphite	[31]	*f*	150	99	1300
SP-1 graphite	[31]	*f*	150	99	1300
SP-1 graphite	[31]	*f*	150	87	1700
SP-1 graphite	[31]	*f*	150	78	2000
SP-1 graphite	[31]	*f*	150	75	2100
SP-1 graphite	[31]	*f*	150	87	1700
SP-1 graphite	[31]	*f*	150	75	2100
SP-1 graphite	[31]	*f*	150	78	2000
SP-1 graphite	[31]	*f*	150	75	2100
SP-1 graphite	[31]	*f*	150	66	2400
SP-1 graphite	[31]	*f*	150	54	2800
SP-1 graphite	[7]	*f*	150	39	3300
Spectroscopic C	[31]	*f*	150	87	1700
Spectroscopic C	[31]	*f*	150	78	2000
Spectroscopic C	[31]	*f*	150	66	2400
Well-crystallised graphite	[19]	*f*	130	88	1000
Well-crystallised graphite	[19]	*f*	130	88	1000
Amorphous C	[32, 33]	*c*	180	111	1900
Glassy C, graphite	[34–36]	*c*	140	38	3000
Kish graphite	[23, 27]	*r*	300	287	25
Fullerite C_{60}	[38]	*r*	200	187	25
	t/s	Diamond type	Size/μm	*F*	*E*/eV atom^{-1}
SP-1 graphite	(5000)	C	< 1	0.3	4.63
SP-1 graphite	3600	C	< 1	0.3	4.58
SP-1 graphite	60	C	< 1	0.3	5.04
SP-1 graphite	(6)	C	< 1	0.3	5.34
SP-1 graphite	(3)	C	< 1	0.3	5.43
SP-1 graphite	2000	C	< 1	0.7	5.43
SP-1 graphite	(12)	C	< 1	0.7	5.46
SP-1 graphite	(300)	C	< 1	0.7	5.87
SP-1 graphite	600	C	< 1	0.7	6.26
SP-1 graphite	150	C	< 1	0.7	6.70
SP-1 graphite	10	C	< 1	0.7	6.91
SP-1 graphite	0.003	C	< 0.1	0.7	5.34
Spectroscopic C	(6000)	C	< 1	0.1	6.03
Spectroscopic C	900	C	< 1	0.1	6.56
Spectroscopic C	300	C	< 1	0.1	7.42
Well-crystallised graphite	0.003	H	< 0.1	0.3	2.41
Well-crystallised graphite	0.003	H	< 0.1	0.7	2.28
Amorphous C	600	C	< 0.1	0.1	6.67
Glassy C, graphite	300	C	< 0.1	0.1	9.54
Kish graphite	3600	H	< 0.1	0.1	0.93
Fullerite C_{60}	1800	C	< 0.1	0.1	0.91

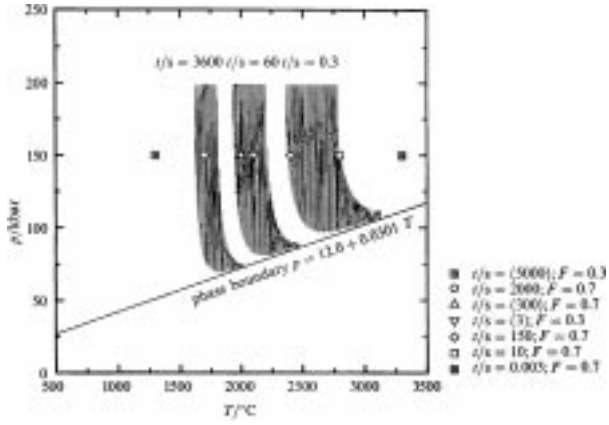

Figure 4 The Kinetic Diagram for the Direct Transition of SP-1 Graphite in Diamond. In the above diagram, experimental data in literature are plotted against three ranges of transition fractions ($F = 0.1$ to 0.9) for different transition times. Numbers labeled are time in seconds.

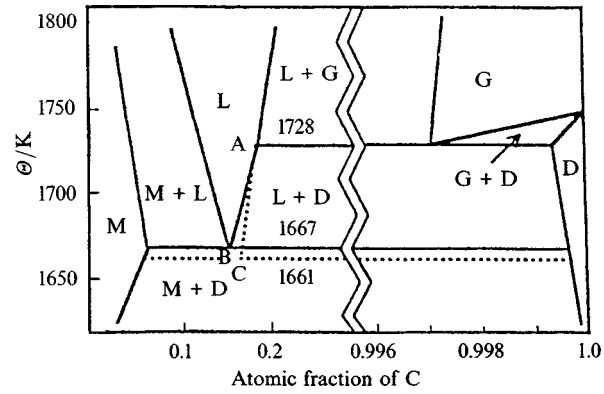

Figure 5 The Phase Diagram of Ni-C at 57 Kb (Strong and Hanneman 1967). In the above diagram, the dotted lines represent the metastable coexistences between graphite and liquid (above eutectic point), and between graphite and metal (below eutectic point). The segment AB is the solubility curve for diamond; and AC, for graphite. L = liquid, M = metal, G = graphite, D = diamond.

It would appear that the kinetics of the direct graphite → diamond transition is highly dependent on the type of graphite used. For example, the transition appears to expedite with the increasing degree of perfection in the original graphite. Thus, the transition rate increases with carbon sources that changes from glassy carbon, amorphous carbon, natural graphite (SP-1) to highly perfect graphite. The degree of conversion (F) of the direct graphite → diamond transition as a function of pressure and time with three transition times (0.3, 30, and 3600 seconds) are plotted in Fig. 4.

5. Kinetics of catalyzed graphite → diamond transition

5.1. The growth of large diamonds

As discussed before, most industrial diamonds are synthesized in a molten metal that serves as a solvent-catalyst. The formation of diamond appears to start with rapid nucleation at the early stage of heating. The nucleation rate tends to decrease with time although it may continue through the entire cycle. Nuclei are typically formed not by supersaturating C atoms from dissolved graphite, but by puckering disintegrated graphite flakes under the catalytic action of solvent-catalyst [9].

Nucleation accounts for a minute proportion of diamond formed. The bulk of transition is proceeded by the growth of existing nuclei. The growth of diamond utilizes the fact that the solubility of the stable diamond phase in the solvent-catalyst is lower than that of the metastable graphite. For example, it has been shown that the difference of solubilities between graphite and diamond in molten nickel at 5.7 GPa is about 1.2 atom% at 1400 °C as shown in Fig. 5 [39]. As a result of this solubility difference, the undersaturated graphite tends to dissolve into the solution; and the supersaturated diamond, deposit onto existing nuclei.

The above solubility difference is achieved at the same temperature. Alternatively, a carbon source, either graphite or diamond, may be placed at a hot end to allow carbon to dissolve to a larger extent. The dissolved carbon can then diffuse toward a cold end where it precipitates out onto a preset seed crystal of diamond. Such a temperature gradient method is often employed

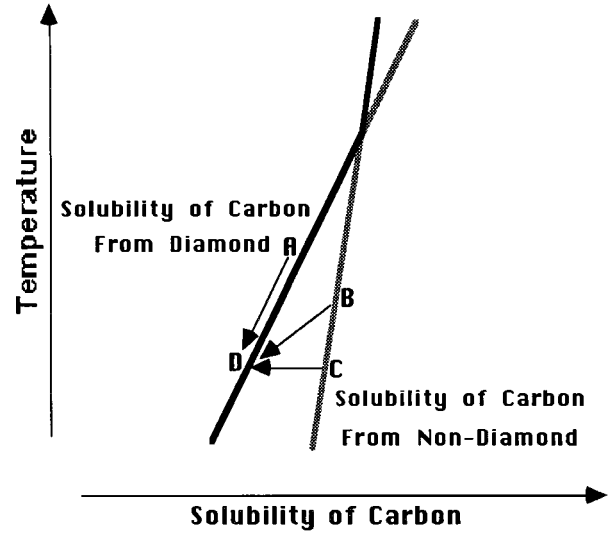

Figure 6 Diamond Growth Routes in Diamond Stability Field. Black lines show the solubility of stable phase in solvent-catalyst; and grey lines, metastable phase. In the diamond stability field (low temperature portion of the above diagram) the solubility of diamond is the lowest among all carbon bearing materials (e.g., the maximum solubility difference between graphite and diamond in Ni at 57 Kb is 0.2 atom%). AD shows the path of temperature gradient method for growing gem diamond on a seeded crystal, using small diamond particles as the nutrient of carbon. CD shows the path of diamond synthesis at constant temperature using typically graphite as the nutrient of carbon. BD is a composite path using both temperature gradient and a non-diamond carbon material for the synthesis.

to grow gem diamond [40]. The comparison of these diamond growth routes is illustrated schematically in Fig. 6.

During the process of growing gem diamond, the pressure window must be maintained very tightly (<0.05 GPa) for extended periods of time. In order to avoid the pressure decay due to the volume reduction of the graphite → diamond transition, the nutrient of carbon used is often diamond fines instead of graphite. Table II lists some historical milestones of gem diamond grown by the temperature gradient method. It would appear that the approximate growth rate of gem diamond may be represented by:

$$L(\mu) = 2052 + 0.00458t(\text{sec}), \text{ or about } 17\mu/\text{hr}.$$

TABLE II Historical synthetic gem diamonds

M (g)	*d* (cm)	*t* (h)	*G* (mg/h)	*G* (μ/h)	Producer	Year	Ref.
2.84	1.03	500	6	21	De Beers	1992	[41]
1.80	0.88	120	15	73	Sumitomo	1990	[42]
0.60	0.61	200	3	33	Gen. Elect.	1990	[43]
0.17	0.40	85	2	47	Gen. Elect.	1971	[44]
0.03	0.23	15	2	150	NIRIM	1981	[45]

The industrial diamonds contains more defects (mainly metal inclusions) than gem diamond. The strongest industrial diamonds with the least defects are often used for the most severe applications such as sawing or drilling rocks or concretes. The saw-grade diamonds represent the largest group of all industrial diamonds. They account for over 80 metric tons of world consumption (over half a billion U.S. dollars) each year. The sizes of high-quality saw-grade diamonds typically range from 18 U.S. mesh (1 mm or 1,000 μ) down to 60 U.S. Mesh (1/4 mm or 250 μ).

The catalyst system used by various diamond manufacturers may be analyzed from their products. It is known that heating these diamonds up to 1400 °C under an inert atmosphere could induce extensive cracks. Moreover, the included catalyst metal will melt and extrude out to the surface to form blisters. By analyzing these blisters the composition of the catalyst used can be deduced [46]. For example, saw-grade diamonds are often grown in a molten alloy of Fe-Ni for General Electric's MBS products [47]; Fe-Co for De Beers SDA products, and more recently Fe-Ni for SDB products; or Fe-Ni-Mn for many Chinese or Russian products.

The saw-grade diamonds can be grown either with or without preplanted diamond seeds. In the former case, the transition proceeds by growing on the existing seed crystals. In the later case, diamond nuclei must form spontaneously. However, as discussed above, the nucleation rate often tapers off with time so the dominant mode of diamond synthesis is also the growth of existing nuclei.

It is assumed that diamond nuclei would grow up to an average size of about 105 μ (U.S. mesh 140) when they become saturated, i.e., nucleation sites are exhausted. Moreover, it is further assumed that the growth time for a high-grade saw diamond crystal of 30/40 mesh size (average size about 0.5 mm) is about half an hour. Based on such assumptions, the growth rate of high-grade sawing diamonds may be represented by:

$$L(\mu) = 105 + 0.217t(\text{sec}) \text{ or about } 780\ \mu/\text{hr}.$$

The melting point of a metal is significantly reduced by its solution of carbon. For example, by dissolving carbon in nickel at 57 Kb, the eutectic melting point is depressed 128 °C, from 1455 °C to 1327 °C (Fig. 5). Some relevant temperature changes due to the mutual solubility of carbon and solvent-catalyst are listed in Table III. The temperature for graphite → diamond transition is also reduced by the solution of metal in carbon. For example, by dissolving Ni in carbon at 57 Kb, the equilibrium transition temperature is suppressed 42 °C, from 1497 °C to 1455 °C (Fig. 5).

5.2. The parameters used in the calculation

If we assume that nucleation is random and it is formed homogeneously inside the molten metal, then the kinetic equation for growing saw diamond may be calculated based on Equation 1. In the early stage of the phase transition when nuclei are continuously forming, such an assumption is valid. Based on many catalogues of diamond producers (e.g., from China), it is found that in a typical run for growing saw diamond, in order to avoid the mutual interference of the growth, the amount of diamond is often kept less than 2 carats/cm^3. This amount of diamond implies that the degree of transition is about $F = 0.1$.

In the following calculations, we have assumed that homogenous nucleation occurs up to a stage of $F = 0.01$, i.e., about one tenth of the final degree of transition. Moreover, the strain energy (ξ) in Equation 11 is neglected as the nuclei is surrounded by the molten alloy that cannot sustain any strain.

The composition of the catalyst is assumed to be similar to Invar, i.e., Fe(65 wt%)-Ni(35 wt%) [48, 49]. The melting curve of the eutectic point, Ni-Fe-C may be found in Table III. The parameters for calculating the kinetics of the graphite → diamond transition for the growth of saw-grade diamond before the exhaustion of nucleation sites are as follows:

$$\begin{aligned} P &= 5\ \text{GPa} \quad (\Delta P = 0.2\ \text{GPa}) \\ T &= 1280\ ^\circ\text{C} \\ t &= 300\ \text{sec} \quad (5\ \text{minutes}) \\ F &= 0.01 \\ n &= 1200/\text{cm}^3 \\ N &= 4/\text{cm}^3 - \text{sec} \\ G &= 0.2\mu/\text{sec} \end{aligned}$$

The activation volume for carbon diffusion in an iron catalyst was found to be about 1 cm^3/mole [44] as

TABLE III Melting points of catalysts (°C)

System	1 atm	57 Kb	ΔT	°C/Kb
Fe	1538	1740	202	3.5
Fe-C	1153	1345	192	3.4
ΔT	−385	−395		
Co	1495	1687	192	3.4
Co-C	1320	1512	192	
ΔT	−175	−175		
Ni	1455	1666	211	3.7
Ni-C	1327	1394	67	1.2
ΔT	−128	−272		
Fe-Ni(35)	1425			
Fe-Ni-C	1040	1057	17	0.3
ΔT	−385			
Ni-Cr(50)	1345			
Mn	1242	1495	253	4.4
Mn-C	1230	1300	70	1.2
ΔT	−12	−195		
Cu	1085	1290	205	3.6
Cu-C	1100	1300	200	3.5
ΔT	15	10		
P	44	1127	1083	19

TABLE IV Calculated surface energy (σ) and activation energy (E_a)

Catalyst	P (kb)	T (°C)	t (sec)	F	σ (erg/cm^2)	σ (eV)*	E_a (eV)
Fe-Ni	50	1200	300	0.01	48	0.007	2.7
Cu	63**	1600	1800	0.001	66	0.010	3.7
$CaCO_3$	77	2150	1200	0.01	126	0.019	4.5
P	77	1800	43200	0.0001	161	0.024	4.9

*σ/the number of atoms on the surface of a diamond nucleus. The surface area of each atom is assumed to be $(1.54)^2 = 2.37$ Å^2.
**The original pressure reported was 60 Kb with an overpressure about 3 Kb. As our model assumes a different phase boundary, the pressure is adjusted to maintain the same overpressure.

determined based on the rate of decreasing carbon's diffusion coefficient at high pressure. This activation energy is adapted in our model (Equation 13).

Based on the above parameters, the interface energy for diamond nucleation and the activation energy for diamond growth are calculated with the result listed in Table I.

6. Kinetics of metal-solvent assisted transition

6.1. The dispute of catalysts

The original list of catalysts for diamond synthesis discovered by General Electric scientists in 1955 include nine Group VIIIa elements (Fe, Co, Ni, Ru, Th, Pd, Os, Ir, Pt) and three other transition metals (Mn, Cr, and Ta) [5]. Wakatsuki [50] found certain non-catalysts, when combined, also show catalytic effect. Specifically, when any of carbide formers of Group IVa, Va, VIa (Ti, Zr, Hf, V, Nb, Mo, or W) is alloyed with Group Ib (Cu, Ag, or Au) elements, diamond could be formed at 60 to 70 Kb and 1500–2000 °C. Fig. 7 shows that when two such non-catalysts in the system of Cu-Nb, when alloyed, could exhibit the catalytic effect [12]. Moreover, it was found that Cu alone could also catalyze the diamond formation when heated by a direct current. The diamond was formed in molten cooper when the sample was held at 67 Kb and heated to 1670 °C for 15 minutes. But when heated in an alternative current at 70 Kb to 1800 °C for the same period of time, no diamond was found [51].

Wakatsuki's claim that copper could trigger diamond formation was discounted by General Electric's Bundy who asserted that the copper used by Wakatsuki could have been contaminated by a catalytic metal. Bundy pointed out that a minute amount of nickel, even as small as 1 wt%, when alloyed with copper, could trigger the nucleation of diamond [52].

However, it has been demonstrated recently that diamond seeds could indeed grow in molten Cu, Zn, Ge, all "non-catalysts." The conditions for this growth was 60 Kb and 1600 °C. For example, when held in molten copper, a tiny diamond seed could grow about half a micron in 5 hours. However, no growth was detected when the temperature was lower than 1400 °C. Most diamond syntheses using traditional catalysts were performed below this temperature.

Moreover, when held at the above conditions for half an hour, small diamond crystals of a few tens microns in size could form spontaneously in molten copper. The copper used in the experiment was analyzed by inductively coupled plasma (ICP) emission spectroscopy and found to contain only 100 ppm of Fe and 10 ppm each of Ni, Co, and Zr. These low levels of impurities should not have caused any noticeable catalytic effect on the graphite → diamond transition [53]. Thus, although not effective, it seems certain that copper can catalyze

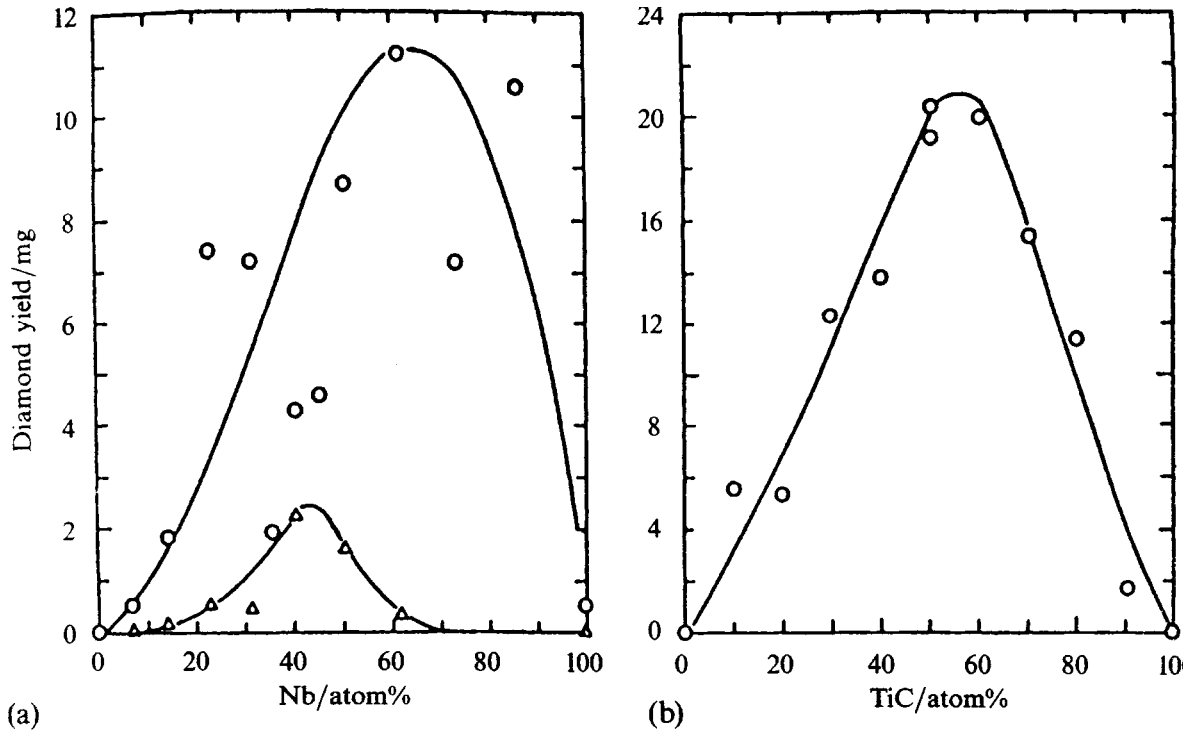

Figure 7 The Catalytic Effect of an Alloy made of two Non-Catalysts (Wakatsuki 1976). Note that Cu, Nb, and TiC individually are not capable to catalyze the diamond formation below a temperature of about 1600 °C. However, when Cu is alloyed with Nb or TiC, the solution behaves like a catalyst similar to Group IIIa metals.

diamond formation at a temperature higher than normally adapted to synthesize diamond using traditional catalysts made of group VIIIa metals.

If the growth rate of diamond in a copper solution is assumed to be 0.02 μ/sec (36 μ in 30 minutes) and $F = 0.001$, the surface energy for nucleation and activation energy for growth can be calculated and the results are listed in Table IV. From these energy barriers, the kinetic equation for the graphite → diamond transition in a copper solvent at the early stage of transition can be obtained from Equation 1.

7. Kinetics of non-metal solvent assisted transition

7.1. The catalytic effect of phosphorous

In addition to copper, many previous "non-catalysts" have been found capable to catalyze the graphite → diamond formation. These "catalysts" may include even non-metals. For example, barium carbide was used as a solvent for synthesizing diamond, and the reaction was found accelerated with the addition of metal borides [54].

One of these non-metal "catalysts" is phosphorous. For example, when graphite was pressed against phosphorous that contained a diamond seed of about 1 mm, and the charge was held at 65 Kb and 1800 °C for 12 hours, the diamond seed could gain 10 wt% (about 30 microns in thickness). Furthermore, diamond nuclei could form spontaneously without seeding in molten phosphorous when the charge is held at 7.7 GPa and 1800 °C for 10 minutes. In contrast to phosphorous, molybdenum appeared to have no effect on graphite when held at the same conditions [55].

The kinetic equation for the nucleation of diamond in molten phosphorous is calculated based on a growth rate of 0.0007 μ/sec (30 μ in 12 hours) and $F = 0.0001$ (it corresponds a length fraction of about 5% that is highly visible). The calculated surface energy of nucleation and the activation energy of growth are listed in Table IV.

7.2. The catalytic effect of carbonates

In addition to phosphorous, many salts of concentrated acids were also found to be capable to convert graphite to diamond. For example, when carbonates (20 V%) of Li, Na, Mg, Ca, or Sr were mixed with graphite and held at 7.7 GPa and 2150 °C for about twenty minutes, all graphite was found to convert to diamond. When the temperature was lowered to 2000 °C, the conversion was about half.

Without the presence of these carbonates, graphite remained unchanged under the same conditions. However, when temperature was lowered to 1800 °C, no diamond was detected even with the presence of these carbonates [56].

The capability of $CaCO_3$ to catalyze the diamond formation is further evidenced by its ability to sinter diamond micron powder at 7.7 GPa and 2200 °C to form a polycrystalline diamond (PCD) body [57].

According to Akaishi *et al.* [56], the diamond crystallite that grew in molten $CaCO_3$ at 2000 °C for 20 minutes was 20 μ in size. Hence the growth rate was about 0.017 μ/sec. The activation energy for this growth rate is calculated to be about 4.5 eV. Moreover, it would appear that the threshold transition temperature for carbonate is around 1900 °C. Based on such an assumption, the interface energy is calculated and listed in Table IV.

In addition to carbonates, sulfates and hydroxides are also found capable of converting graphite to diamond at high pressure and high temperature. Thus, when held at 77 Kb and 2150 °C, diamond was found embedded in a powder mixture of graphite with 20 V% of Na_2SO_4, $MgSO_4$, $CaSO_4.1/2H_2O$, $Mg(OH)_2$, or $Ca(OH)_2$. Again, without the presence of such salts, graphite would not transform to diamond under the same conditions [58].

Further studies indicates that the minimum conditions for synthesizing diamond in the system of graphite-$CaSO_4$ was 7.7 GPa and 1700 °C, or 7 GPa and 2000 °C [59]. Such results are not contradictory to the lower temperature diamond syntheses of early General Electric Company. According to the latter, graphite in contact with chlorides, oxides, sulfides, and carbonates could only yield exsolved graphite at 60 Kb and 1600 °C [60].

8. Discussions

8.1. The effect of graphite on transition

It is well known that diamond synthesis is highly dependent on both graphite and catalyst. In the case of graphite, there is a general tendency of lowering the nucleation temperature with the increasing degree of graphitization. Moreover, graphite is the necessity form for the nucleation of diamond, so amorphous carbon must first graphitized before any diamond can be formed [61]. Thus, graphitizable carbon such as carbon black (microscopic crystallites of graphite) and coke (large grains of graphite) are more readily convertible to diamond [61]. Amorphous carbon, when combined with a suitable catalyst, has also been shown incapable of nucleating diamond in the pressure and temperature region where graphite can [62]. So was pure carbyn, the linear form of carbon [63, 64].

The kinetic model for the direct graphite → diamond transition appears to follow the same tendency. Thus, the activation energy and hence the threshold temperature for the transition are decreasing in the order from amorphous glassy carbon, poorly graphitized spectroscopic carbon, naturally occurred graphite (SP-1), to well-crystallized graphite (Table I). As the separation between basal planes decreases with the increasing degree of graphitization, it appears that the decrease of this separation is directly responsible for the reduction of the activation energy and threshold temperature for the direct graphite → diamond transition.

Kish graphite is exsolved carbon that segregates out from a molten iron. It contains intercalated iron atoms that are located in hexagonal sites between two graphite layers. As a result, these layers are pulled closer so the separation of graphite layers in kish is actually lower than even that of Ceylon's natural graphite, the best of all graphites [65]. Therefore, the iron-impregnated graphite has an even lower activation energy as well as threshold temperature.

Fullerene (C_{60}) is another type of "graphite" that is partially diamond-like The carbon bonds have a mixed characteristics of $sp^2\pi$ and sp^3. Therefore, the activation energy and threshold temperature for its transition to diamond are also lower than that of normal graphite.

According to Table I, the activation energies for the direct graphite → diamond transition range from over 2 eV for perfect graphite to nearly 10 eV for glassy carbon. These energies may be compared with certain relevant bond energies. The energies for breaking a van der Waal bond, a sp^3 diamond bond, and a $sp^2\pi$ graphite bond are 0.076 eV, 3.69 eV, and 4.77 eV, respectively. It would appear that most direct transitions of graphite → diamond would require breaking $sp^2\pi$ bonds. However, with well crystallized graphite, it may require breaking fewer than half of these bonds. When kish graphite or fullerene are used, the activation energy is further lowered.

8.2. The effect of catalyst on transition

In addition to graphite, the kinetics of the graphite → diamond transition is highly dependent on the catalytic power of a solvent. The original General Electric patents on diamond synthesis call for the use of "catalysts" made of certain transition metals [5]. The catalytic interpretation of these metals were challenged by De Beers during their patent dispute. De Beers, who purchased ASEA's diamond technology in 1965, maintained that diamond was formed by a solution mechanism. A similar view was held by others [66, 67]. As discussed before, Bundy and Wakatsuki also argued about whether copper was capable to form diamond or not.

The catalytic power of a solvent for the graphite → diamond transition is best manifested in its ability to lower its interface energy with diamond. General Electric scientists suggested such a possibility but provided no evidence [68, 69]. Subsequently, Russians pointed out that the catalytic effect is equivalent to a decrease of interface energy as high as two orders of magnitude [70]. There is no known mechanism to account for such a large drop of interface energy. Our results (Table IV) indicate that the decrease of interface energy is indeed enormous, nearly two orders of magnitude for traditional catalysts (Group VIIIa elements) as Russians predicted. However, the decrease of interface energies are much less dramatic for lesser catalysts.

Diamond has the highest surface energy of all materials. The calculated surface energies for a freshly cleaved plane are 5300 erg/cm^2 for (111) plane, 6500 erg/cm^2 for (110), and 9200 erg/cm^2 for (100) plane [71]. The measured surface energy with its vapor was 3700 erg/cm^2 [72]. The interface energy is lowered by the contact of a molten metal. The higher carbon solubility of a solvent is, the lower its interface energy with diamond may be. However, even so, all interface energies measured at ambient pressure are higher than 2000 erg/cm^2.

8.3. The decrease of interface energy

When a diamond crystal is formed from a catalyst-solvent, it is always enclosed by a thin metal film. As the diamond crystal grows, this metal film will expand like a balloon. However, despite the enlargement of the metal film, its thickness remains at about 0.1 mm [73].

It is known that carbon solubility will increase with increasing pressure. For example, carbon solubility in Ni at ambient pressure is 2.7 atom%. It increases to 11.6 atom% at 5 GPa [74]. Moreover, it was found that in the metal (Fe or Ni) skin that surrounds a diamond crystal, the carbon content could be enriched to a level as high as 75 atom% [75]. The unusual enrichment of carbon in the metal skin that surrounds a diamond crystal can dramatically decrease the interface energy and hence facilitate the diamond nucleation.

The dissolved carbon atoms may enter either octahedral or tetrahedral interstitial sites of the molten alloy. It was found that at high pressure, carbon atoms in a metal skin that surrounded diamond were in tetrahedral sites. Moreover, they formed a diamond-like structure (sphalerite) with the host metal. In fact, the lattice parameter of this structure was found to be close to that of diamond itself [76]. Such a high enrichment of carbon in metal and the close resemblance of structural parameters between this metal skin and diamond can undoubtedly minimize the surface tension. Therefore, the two-order magnitude decrease of interface energy between the metal skin and diamond is explained.

Recently, the Penn State scientists have discovered that many molten metals can also dissolve substantial amount of carbon when they are saturated with hydrogen atoms. These metals normally do not dissolve much carbon at ambient pressure without the presence of hydrogen atoms. As a result of the large dissolution of both carbon and hydrogen, the melting points of these solvents can be dramatically depressed below their normal eutectic points. In fact, such a new phenomenon has been used to synthesize diamond metastably in a liquid phase under ambient pressure [10, 11].

For example, the solubility of carbon in molten silver is negligible. However, with the incorporation of a large amount of hydrogen atoms, the solubility of carbon can surge up to about 70 atom%. As a result, the eutectic point is plunged from 962 °C to 750 °C. Thus, although silver is normally not a catalyst for the graphite → diamond transition under high pressure, it becomes one even at ambient pressure with the incorporation of a large amount of hydrogen atoms [77]. It is believed that the simultaneous incorporation of carbon and hydrogen atoms can allow the interstitial solution of CH_4-like clusters in the solvent. As a result, the overall free energy can be lowered than that of normal eutectic compositions. The CH_4-like clusters can facilitate the diamond formation in a liquid phase just as CH_4 can in a gas phase [11].

The activation energies of growth for the solvent-assisted graphite → diamond transition tend to correlate with their activation energies of nucleation. This correlation suggests that both types of activation energies are determined by the common factors of crystal chemistry. A comprehensive review of these factors are presented elsewhere [9, 11].

It is known that the catalyst for the graphite → diamond transition is also the catalyst for the reverse transition at ambient pressure. The activation energies for the catalytic graphitization of diamond are 3.3 eV for

Fe, 3.4 eV for Co, and 5.0 eV for Ni [78]. These activation energies appear to be higher than that (Table IV) for the corresponding graphite → diamond transition.

9. Conclusions

Our kinetic models suggest that all carbon solvents in liquid form have various degrees of effectiveness in catalyzing graphite → diamond transition. The effectiveness of a catalyst is inversely proportional to its activation energy of both nucleation and growth (Table IV). Hence, Fe or Ni is a much more powerful catalyst than Cu, and the latter is in turn more powerful than P or $CaCO_3$.

The solubilities of carbon at ambient pressure in various solvents that may catalyze the graphite → diamond transition have been analyzed in detail [9]. It would appear that the activation energies calculated according to our kinetic model decrease with the increasing solubility of carbon. Hence, the catalytic power of a solvent is also reflected in its ability to dissolve carbon. Thus, the eutectic (or peritectic, e.g., Cu) composition of carbon at ambient pressure may be a de facto expression of the catalytic power of a solvent [9, 11]. This conclusion may reconcile the half-century long debate between catalytic and solution hypotheses of the graphite → diamond transition. These two mechanisms are governed by the same crystal chemistry – the degree of moderation of metal-carbon reactivity [9]. Hence, they are not contradictory, but representing two sides of the same coin,

Moreover, the easiness for the graphite → diamond transition is greatly affected by the degree of graphitization of the graphite (Table I). Thus, both the degree of graphitization of carbon source and the degree of carbon solubility of the liquid medium can contribute to "easiness" of diamond synthesis. Hence, the transition of a poorly graphitized carbon, e.g., a glassy carbon, in an effective catalyst, e.g., an alloy of Fe-Ni, may not be easier than that of a highly graphitized graphite, e.g., SP-1, in a poor catalyst, e.g., Cu.

The combined effect of carbon source and solution mechanism is evident when we examine the kinetic curves of Fig. 8. For example, although phosphorous can cause a certain graphite to transform into diamond at a lower threshold temperature, its catalytic power cannot match with that of a highly graphitized natural graphite (SP-1) in the direct graphite → diamond transition. Although there were no experimental data available, we can conclude that the threshold temperature for the phosphorous assisted transition of SP-1 graphite could be even lower than that for the direction transition.

The kinetic model described in this research can be used to design a better catalytic system for diamond synthesis [9, 11]. Furthermore, this model may shed the light on the origin of diamond formed in nature. For example, the silicate kimberlite is capable to dissolve a certain amount of carbon. It is estimated that the diamond content in a typical kimberlite pipe is about one carat (1/5 gram) for every 5 tons of rock, or a concentration of about 4×10^{-8}. If we assume that the activation energy for the conversion of diamond in kimberlite is as small as that for non-metal catalysts, e.g., P and $CaCO_3$ (Table IV), it is possible to calculate the kinetic curve (F as a function of P, T, and t) for the formation of natural diamond in kimberlite. As kimberlite pipes can trace its origin to 200 Km deep where the pressure is about 60 Kb and the temperature is about 1200 °C. From these parameters, it is possible to estimate that the possible time required for the formation of natural diamond. The result indicates that the precipitation of natural diamond out of kimberlite might take only a few years. This time frame is an instant moment when compared with hundreds of thousands years that may be needed to solidify a molten kimberlite.

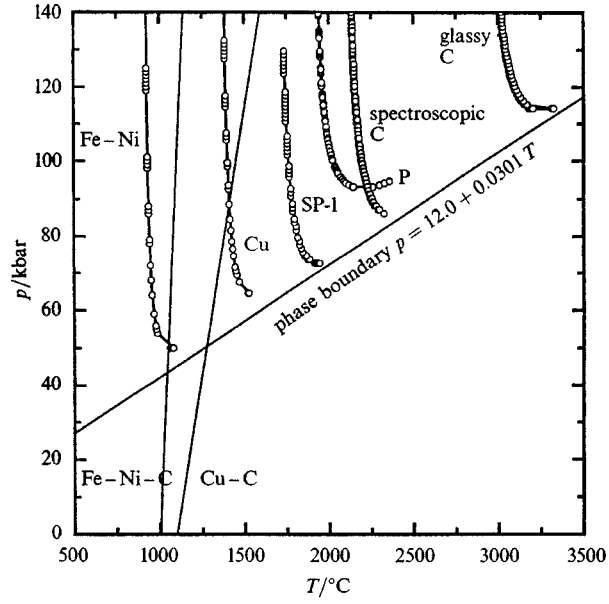

Figure 8 Kinetic Curves of Graphite → Diamond Transition. The diagram includes both direct transitions and solvent-assisted transitions. In the later case, the curve below the melting point of the solvent is shown only as reference. The diamond formation is impossible in this region because activation energy would rise drastically when the solvent solidifies. Note these curves appear to be limited by vertical threshold temperatures. If the activation volume is larger than assumed (1 cm^3/mole), these curves will bend toward higher temperatures above a threshold pressure.

References

1. C. M. SUNG and M. SUNG, *Materials Chemiistry and Physics* **43** (1996) 1.
2. J. W. MELLOR, "Comprehensive Treatise on Inorgainc and Theroetical Chemistry, Vol. 5" (Longmans Green & Co., 1924).
3. H. LIANDER, *ASEA J.* **28** (1955) 97.
4. H.T. HALL, *The Chemist* (1970) 276.
5. F. P. BUNDY, H. T. HALL, H. M. STRONG, R. H. WENTORF JR., *Nature* **176** (1955) 51.
6. P. S. DECARLI and J. C. JAMIESON, *Science* **133** (1961) 1821.
7. F. P. BUNDY, *J. Chem. Phys.* **38** (1963) 631.
8. H. M. STRONG and R. H. WENTORF JR., *Naturwissenschaften* **59** (1972) 1.
9. C. M. SUNG and M. F. TAI, *High Temp.-High Press*, in press.
10. C. M. SUNG and M. F. TAI, *J. Refractory Metals and Hard Materials* **15** (1997) 237.
11. C. M. SUNG and M. F. TAI, High Temp.-High Press, submitted.
12. M. WAKATSUKI, Ph.D. dissertation, 1976.
13. K. CHENG, *Scientia Sinica* **16** (1973) 336.
14. J. W. CAHN, *Acta Met.* **4** (1956) 449.

15. C. M. SUNG, in Proc. 6th AIRAPT International High Pressure Conf. (1978) p. 31.
16. A. V. KURDYUMOV, *Sov. Phys. Dold.* **20** (1975) 218.
17. S. FAHY *et al., Phys. Rev.* **B34** (1986) 1191.
18. R. M. WENTZCOVITCH *et al., Physical Review* **B38** (1988) 6191.
19. F. P. BUNDY and J. S. KASPER, *J. Chem., Phys.* **46** (1967) 3437.
20. R. G. BURNS and C. M. SUNG, *Phys. Chem. Minerals* **2** (1978) 349.
21. S. FAHY and S. LOUIE, *Phys. Rev.* **B36** (1987) 3373.
22. W. UTSUMI *et al.,* (1994).
23. T. YAGI *et al., Physical Review* **B46** (1992) 6031.
24. C. M. SUNG and M. F. TAI, *High Temperatures–High Pressures* **29** (1997) 631.
25. JI-AN XU, personal communications (1996).
26. R. BERMAN, in "Properties and Growth of Diamond," edited by G. Davies (Short Run Press, Exeter, England, 1994) p. 30.
27. C. S. KENNEDY and G. C. KENNEDY, *J. Geophys. Res.* **81** (1976) 2467.
28. F. BIRCH, *Phys. Rev.* **71** (1947) 809.
29. *Idem., J. Geophys. Res.* **57** (1952) 227.
30. *Idem., ibid.* **83** (1978) 1257.
31. WENTORF, (1965).
32. ONODERA *et al.*, (1988).
33. *Idem.*, (1991).
34. NAKA *et al.*, (1976).
35. HIRANO *et al.*, (1982).
36. NAKA *et al.*, (1981).
37. UTSUMI and YAGI, (1991).
38. REGUEIRO *et al.*, (1992).
39. H. M. STRONG and R. E. HANNEMAN, *J. Chem. Phys.* **46** (1967) 3668.
40. R. H. WENTORF JR., *J. Phys. Chem.* **75** (1971) 1833.
41. R. J. CAVENEY, *Mater. Sci. Eng. B (Switzerland),* **11** (1992) 197.
42. H. SUMIYA *et al.*, in 31st High Pressure Conf., Japan, 1990, p. 48.
43. S. VAGARALI *et al., J. Hard Mater. (UK),* **1** (1990) 233.
44. H. M. STRONG and R. M. CHRENKO, *J. Phys. Chem.* **75** (1971) 1838.
45. H. KANDA *et al., J. Chem. Soc. Japan* **9** (1981) 1349.
46. V. G. GARGIN, *Sverkhtverd. Mater.* **2** (1982) 17.
47. S. K. DICKINSON JR., Air Force Cambridge Research Laboratories, Physical Sciences Research Papers, No. 434 (AFCRL-70-0628) 1970.
48. H. P. BOVENKERK, U.S. Patent 2,992,900 (1961) Example 1.
49. *Idem.,* U.S. Patnet 3,083,080 (1963) Example 4.
50. M. WAKATSUKI, *Japan. J. Appl. Phys.* **5** (1966) 337.
51. M. WAKATSUKI *et al.*, in Proceedings of the 4th International Conference on High Pressure, Kyoto, Japan, (1974) edited by J. Osugi *et al.*, p. 413.
52. F. P. BUNDY, *Nature* **241** (1973) 116.
53. H. KANDA *et al., Appl. Phys. Lett.* **65** (1994) 784.
54. T. KURATOMI U.S. Patent 3,737,903 (1973).
55. M. AKAISHI *et al., Science* **259** (1993) 1592.
56. M. AKAISHI *et al., J. Crystal Growth* **104** (1990) 578.
57. M. AKAISHI *et al., J. Hard Mater.* **3** (1992) 75.
58. M. AKAISHI *et al., Japanese J. of Appl. Phyiscs* **29** (1990) L1172.
59. M. AKAISHI *Diamond and Related Materials* **2** (1993) 183.
60. R. H. WENTORF JR. *Ber. Bunsenges. Phys. Chem.* **70** (1966) 975.
61. V. I. KASATOCHKIN, L. E. SHTERENBERG, V. N. SLESAREV and Y. N. NEDOSHIVIN, *Dokl. Akad. Nauk SSSR* **194**(4) (1970) 801.
62. R. H. WANG, K. T. WANG and J. W. HSU, in Synthesis Mechanism of Artificial Diamond Conference, Jeng-Zhou, China, 1973.
63. V. I. KASATOCHKIN *et al., Dokl. Akad. Nauk SSSR* **177** (1967) 358.
64. V. I. KASATOCHKIN, *ibid.* **209** (1973) 388.
65. P. S. WALKER, *Nature* **180** (1957) 1185.
66. H. J. RODEWALD, *Chimia* **15** (1961) 251.
67. Y. A. LITVIN, *Neorganicheskie Materialy* **4** (1968) 175.
68. H. P. BOVENKERK *et al., Nature* **184** (1959) 1094.
69. H. M. STRONG, *J. Chem. Phys.* **39** (1963) 2057.
70. D. V. FEDOSEEV and B. V. DERYAGIN, *Dokl. Akad. Nauk SSSR* **238**(1) (1978) 91.
71. H. O. PIERSON, "Handbook of Carbons, Graphite, Diamond and Fullerenes" (Noyes, Park Ridge, New Jersey, 1993).
72. B. V. BELOKUROV, *Zh. Fiz. Khim.* **34** (1960) 440.
73. R. H. WENTORF JR., *Chem. Technik* **12** (1960) 531.
74. H. M. STRONG, *Trans. AIME* **233** (1965) 643.
75. A. A. GIARDINI and J. E. TYDINGS, *Am. Mineral.* **47** (1962) 1393.
76. K. LONSDALE, H. E. MILLIDGE and E. NAVE, *Miner. Mag.* **32** (1959) 246,185 .
77. R. ROY *et al.*, in Applications of Diamond Films and Realted Materials: Third International Conference, 1995, edited by A. Feldman *et al.*, p. 391.
78. P. H. CLIFTON and S. EVANS, *Indus. Diam. Res.* **1/95** (1995) 26.

Received 22 May 1996
and accepted 15 March 2000